

## Structure of Liquid Films of an Ordered Foam Confined in a Narrow Channel

Emmanuel Terriac,<sup>†</sup> Franck Artzner,<sup>†</sup> Alain Moréac,<sup>†</sup> Cristelle Meriadec,<sup>‡</sup> Patrick Chasle,<sup>†</sup> Jean-Claude Ameline,<sup>†</sup> Jérémy Ohana,<sup>†</sup> and Janine Emile<sup>\*,†</sup>

Groupe Matière Condensée et Matériaux, UMR CNRS 6626, Université de Rennes I, Campus de Beaulieu, 35042 Rennes Cedex, France, and Sciences Chimiques de Rennes, Ecole Nationale Supérieure de Chimie de Rennes, UMR 6226, Campus de Beaulieu, 35700 Rennes Cedex, France

Received June 13, 2007. In Final Form: September 6, 2007

A bamboo foam is the simplest case of an ordered foam confined in a narrow channel. It is made of a regular film distribution, arranged perpendicularly to the channel. Our work consists of studying the structural properties of several films taken in a drained foam. X-ray experiments highlighted the equality of the equilibrium thickness for each film within a foam. The same thickness was found as by measurements of disjoining pressure isotherms, proving as well that films of a bamboo foam behave like isolated ones. The refinement of X-ray data by a simple model of specular reflectivity showed a significant variation of the electronic distribution of the surfactant layer for a common black film forwarding from one equilibrium state to another. A discussion on the organization of the surfactant molecules to the gas/liquid interface and film is proposed.

### Introduction

Aqueous foam is a dispersion of gas bubbles separated by thin liquid films, stabilized by surfactant molecules.<sup>1</sup> Liquid films are formed between two adjacent gas bubbles, and Plateau borders (channels) are formed where three neighboring films meet. In a three-dimensional foam (3D), the structure is generally disordered. However, ordered foams can be generated in confined media such as porous materials<sup>2,3</sup> or microchannels.<sup>4–6</sup> The simplest structure corresponds to the bamboo foams formed by an equal spacing of parallel films. This can be generated in a tube, whose bubbles are identical and of a size close to the one of the diameter of the tube.<sup>7,8</sup> According to the orientation of the tube (vertical or horizontal), one distinguishes two categories of liquid films: films perpendicular to the wall of the tube and the wetting film. The junction between them is ensured by the Plateau border corresponding here to a meniscus surrounding the circumference of the tube. Various theoretical and experimental studies were undertaken in bamboo foams flowing through directed narrow channels.<sup>9,10</sup> Rheological information is extracted from it for understanding the foam–wall friction. According to the surface shear rheology, the viscous dissipation occurs inside the Plateau borders and mainly in the wetting film.<sup>11,12</sup> Collective

dynamics is thus managed by the wetting film. With regard to the static case of the foam, the collective aspect does not seem clearly defined. Experiments about the drainage (flow of liquid through foam) have shown an unusual behavior:<sup>13</sup> the shape of the Plateau border cross-section can strongly influence the flow in the wetting film. In the extreme case (tube radii less than  $0.918l_c$ ,  $l_c$  capillary length of the foam solution), the drainage is not observed and the wetting film does not seem to ensure anymore the connection between various films constituting the bamboo foam. A fundamental question results: is foam bamboo a succession of independent films or not?

The main motivation of our study is to investigate the structural properties of bamboo foams, which constitute a stable configuration. The coarsening (gas diffusion) of a completely disordered foam inside a narrow tube leads to the development of a bamboo foam.<sup>14</sup> Recent experiments performed by A. Le Goff and D. Quéré revealed that this type of foam can stop solid particles without making burst films, which constitutes a useful tool to study the kinetic energy absorption properties in aqueous foams. In such a context, we have performed small-angle X-ray scattering experiments on bamboo foams of SDS (sodium dodecyl sulfate), whose physicochemical properties are well-known. In particular, we selected a film among the series of films to extract its structure (thickness and configuration of the surfactant molecules of SDS to the interface gas/liquid and in film). In parallel, experiments using the thin film pressure balance apparatus were carried out on a single film under compression to reach the state of common black film. Disjoining pressure isotherms were measured and compared to the X-ray results, to understand the relation possibly existing between an isolated film and a single film taken randomly in a bamboo foam.

### Experimental Section

**Materials.** All experiments presented here were carried out with solutions of 12 g/L (0.042 M) sodium dodecyl sulfate (SDS;  $\text{CH}_3(\text{CH}_2)_{11}\text{SO}_3^-$ ,  $\text{Na}^+$ ) in pure water. This concentration was far

\* Corresponding author. Tel.: +33 2 23 23 56 46. Fax: +33 2 23 23 67 17. E-mail: janine.emile@univ-rennes1.fr.

<sup>†</sup> Université de Rennes I.

<sup>‡</sup> Ecole Nationale Supérieure de Chimie de Rennes.

(1) Weaire, D.; Hutzler, S. *The Physics of Foams*; Clarendon Press: Oxford, U.K., 1999.

(2) Hirasaki, G. J.; Lawson, J. B. *SPE J.* **1985**, *25*, 176.

(3) Rossen, W. R. Foams in Enhanced Oil Recovery. In *Foams: Theory, Measurements and Applications*; Prud'homme, R. K., Khan, S., Eds.; Marcel Dekker: New York, 1996; Chapter 12.

(4) Hutzler, S.; Weaire, D.; Crawford, R. *Philos. Mag. B* **1997**, *75*, 845.

(5) Drenckhan, W.; Cox, S. J.; Delaney, G.; Holste, H.; Weaire, D.; Kern, N. *Colloids Surf., A* **2005**, *263*, 52.

(6) Raven, J. P.; Marmottant, P.; Graner, F. *Eur. Phys. J. B* **2006**, *51*, 137.

(7) Pittet, N.; Rivier, N.; Weaire, D. *Forma* **1995**, *10*, 65.

(8) Pittet, N.; Boltzenhagen, P.; Rivier, N.; Weaire, D. *Europhys. Lett.* **1996**, *35*, 547.

(9) Cantat, I.; Kern, N.; Delannay, R. *Europhys. Lett.* **2004**, *65*, 726.

(10) Terriac, E.; Etrillard, J.; Cantat, I. *Europhys. Lett.* **2006**, *74*, 909.

(11) Denkov, N. D.; Tcholakova, S.; Golemanov, K.; Subramanian, V.; Lips,

*Colloids Surf., A* **2006**, *282*, 329.

(12) Saugey, A.; Drenckhan, W.; Weaire, D. *Phys. Fluids* **2006**, *18*, 053101.

(13) Carrier, V.; Hutzler, S.; Weaire, D. *Colloids Surf., A*, in press.

(14) Fortes, M. A.; Rosa, M. E.; Findlay, S.; Guedes, M. *Philos. Mag. A* **1998**, *77*, 257.

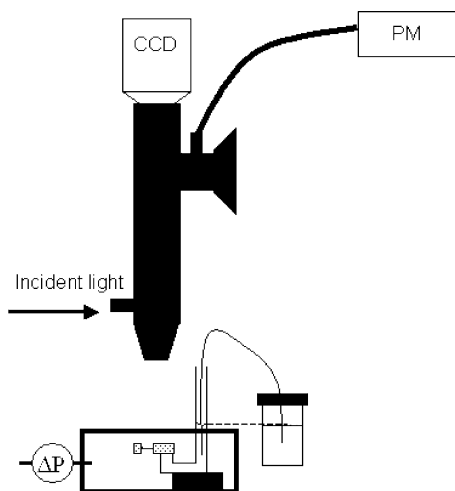


**Figure 1.** Scheme of the thin film pressure balance setup. CCD and PPM refer respectively to CCD camera and photomultiplier.

above the critical micellar concentration of SDS ( $cmc = 2.3 \text{ g/L}^{15}$ ) and was chosen to compare our results with previous ones.<sup>16–18</sup> SDS was purchased from Fisher Scientific Labosi and was used as received (purity higher than 99%). Although it is known that SDS may hydrolyze in non-alkaline medium and produces dodecanol, no further purification process was performed. Both small-angle X-ray scattering (SAXS) and thin film pressure balance (TFPB) experiments were performed with the same lot and on solution prepared less than 12 h before experiment. Surface tension of the solution was measured via the Wilhelmy plate technique and found to be  $35.6 \text{ mN/m}$  at  $22 \text{ }^\circ\text{C}$ .

**Disjoining Pressure Measurements.** Measurements on single films were performed on a home-built TFPB apparatus. Figure 1 describes the experimental setup. The apparatus is very close to ones found in various references.<sup>19–22</sup> The film is supported on a 20 mm diameter drilled porous glass with a diameter of the pores of  $120 \mu\text{m}$ . The hole in which the film is formed is 1.5 mm of diameter. The porous plate is connected to a 4 mm glass tube in which the solution is free to move. This film holder was then placed in a constant gas pressure cell. The pressure within that cell was adjusted by a syringe and controlled by a Keller pressure sensor measuring in the range 0–10 mbar. The reference for the pressure measurement was set on the room pressure, the fluctuations of which were minimized with a glass tank used as a “buffer volume”. To calculate the disjoining pressure of the film, we used the following relation:

$$\Pi = P_g - P_l = \Delta P + 2\gamma/r - \Delta\rho gh_c \quad (1)$$

where  $P_l$  and  $P_g$  are the liquid and gas pressures,  $\Delta P$  is the difference between  $P_g$  and  $P_{\text{ref}}$  (the reference pressure),  $\gamma$  is the surface tension of the surfactant solution,  $r$  is the glass tube radius,  $\Delta\rho$  is the density difference between the solution and air,  $g$  is the gravitational acceleration, and  $h_c$  is the height of liquid within the tube.

Preliminary experiments showed that it was difficult with our apparatus to follow  $h_c$  during the compression of the film. Our tube being quite thin, the height of liquid does not remain constant. This problem was skipped by connecting the liquid in the tube to an external solution reservoir via a rubber capillary tube. Thus, the relevant height becomes the reservoir height relatively to the film.

We used a pot as a reservoir, and then no variation in the liquid height was observed for the studied pressure range. With this setup, we reached a control and an accuracy on the disjoining pressure of less than 2 Pa. The film thickness was determined interferometrically. White light from a 150 W Philips halogen lamp was conducted via a fiber optic cable to a homemade reflected light microscope. After reflection on the film, the light was separated by a beam splitter. One part of the signal was used for direct visualization of the film on a Watec 221-S video color camera. The other part was filtered through a green optical filter (546 nm, bandpass 10 nm) and was collected in a Gamma scientific ocular equipped with a  $450 \mu\text{m}$  optic fiber probe. Hence, we could select the area of the film to be probed during experiment. The intensity of this signal was then measured via a photomultiplier. The film thickness was then determined using equations derived by Sheludko and Plakatnikov<sup>23,24</sup> if we consider a homogeneous refractive index for the film:

$$h = \left(\frac{\lambda}{2\pi n}\right) \arcsin \sqrt{\frac{\Delta}{1 + (4R/(1-R)^2)(1-\Delta)}} \quad (2)$$

where  $h$  is the film thickness,  $\lambda$  is the wavelength of light (546 nm), and  $n$  is the refractive index of the film (about 1.33).  $R$  is the ratio  $(n-1)^2/(n+1)^2$ .  $\Delta$  is a normalization ratio of the light intensity and equals  $(I - I_{\text{min}})/(I_{\text{max}} - I_{\text{min}})$ , where  $I$  is the measured light intensity and  $I_{\text{min}}$  and  $I_{\text{max}}$  are the minimum and maximum intensities of the last interference, which are measured for each experiment.  $I_{\text{min}}$  is determined after film rupture, which sets the light intensity for a zero thickness. The major difficulty in this process was the determination of  $I_{\text{max}}$ . Small fluctuations of the incident light intensity made error bars on film thickness reach 3 nm. The apparatus was situated in an air-conditioned room ( $22 \text{ }^\circ\text{C}$ ) and placed on an optical table to avoid vibrations.

**Small-Angle X-ray Scattering.**<sup>25</sup> X-ray patterns were collected with a Mar345 Image-Plate detector (Maresearch, Norderstedt, Germany) mounted on a rotating anode X-ray generator FR591 (Bruker, Courtaboeuf, France) operated at 50 kV and 50 mA. The monochromatic Cu K $\alpha$  radiation ( $\lambda = 1.541 \text{ \AA}$ ) was focalized with a  $350 \mu\text{m}$  focal spot at 320 mm by a double reflection on an elliptic cross multilayer Montel mirror (Incoatec, Geesthacht, Germany). The beam was defined under vacuum by four motorized carbon-tungsten slits (JJ-Xray, Roskilde, Denmark) positioned in front of the mirror ( $500 \mu\text{m}$ ). Four additional guard slits were placed at the focal point with a 220 mm slit separation distance. The flux after the output mica windows was  $1 \times 10^8$  photons/s. A 3 mm squared lead beam stop was placed under vacuum at 450 mm after the sample, and the detector was positioned at 537 mm. The sample to detector distance was calibrated by using silver behenate. The X-ray patterns were therefore recorded for a range of reciprocal spacing  $q = 4\pi \sin \theta/\lambda$  from  $0.05$ – $0.19 \text{ \AA}^{-1}$  where  $\theta$  is the diffraction angle. The experiments performed with the present setup provide accurate measurements of distances larger than  $30 \text{ \AA}$ .

Samples for SAXS were prepared in a 4 mm diameter Kapton tube, the contribution of which was low in the studied  $q$ -range. The tube was set on the top of a syringe, and a small amount of liquid was poured in it. Foams were obtained by bubbling gently air within the solution and tilting the tube. The bubbling velocity and tilting angle determine the geometry of the foam. Here, we focused on bamboo foam formation. The typical periodicity of the foam, defined by the spacing of films, was slightly more than 2 mm. We estimated the liquid fraction of the foam by weighting just after formation to be around 11% and consider this value as a wet foam. Some experiments were made after shaking the tube to evacuate some water. In that case, liquid fraction has been estimated to be 1% corresponding to the case referred to as “shaken” foams. Both sides of the tube were shut with caps to avoid evaporation during

(15) Rana, D.; Neale, G.; Hornof, V. *Colloid Polym. Sci.* **2002**, *280*, 775.

(16) Axelos, M. A. V.; Boué, F. *Langmuir* **2003**, *19*, 6598.

(17) Etrillard, J.; Axelos, M. A. V.; Cantat, I.; Artzner, F.; Renault, A.; Weiss, T.; Delannay, R.; Boué, F. *Langmuir* **2005**, *21*, 2229.

(18) Terriac, E.; Emile, J.; Axelos, M. A. V.; Grillo, I.; Meneau, F.; Boué, F. *Colloids Surf., A*, in press.

(19) Mysels, K. J.; Jones, M. N. *Discuss. Faraday Soc.* **1966**, *42*, 42.

(20) Exerowa, D.; Scheludko, A. C. R. *Acad. Bulg. Sci.* **1971**, *24*, 47.

(21) Bergeron, V.; Radke, C. J. *Langmuir* **1992**, *8*, 3020.

(22) Stubenrauch, C.; von Klitzing, R. *J. Phys.: Condens. Matter* **2003**, *15*, R1197.

(23) Scheludko, A.; Plakatnikov, D. *Kolloidn. Zh.* **1961**, *175*, 150.

(24) Scheludko, A. *Adv. Colloid Interface Sci.* **1967**, *1*, 391.

(25) Van Grondelle, W.; López Iglesias, C.; Coll, E.; Artzner, F.; Paternostre, M.; Lacombe, F.; Cardus, M.; Martinez, G.; Montes, M.; Cherif-Cheikh, R.; Valéry, C. *J. Struct. Biol.* **2007**, *160*, 211.

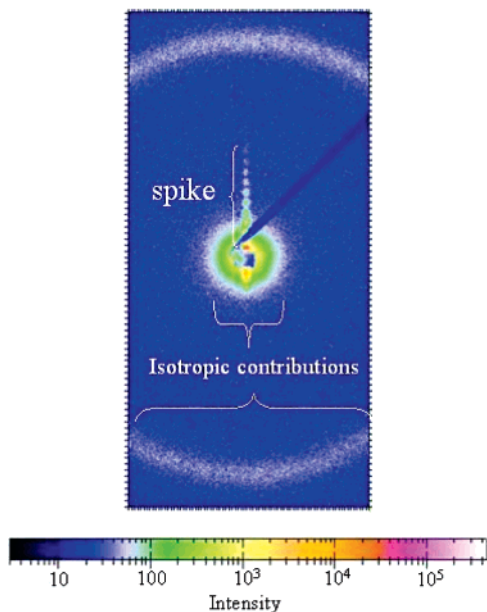


**Figure 2.** Example of a SAXS pattern recorded for a 17 nm SDS foam film (visualization by FIT2D software).

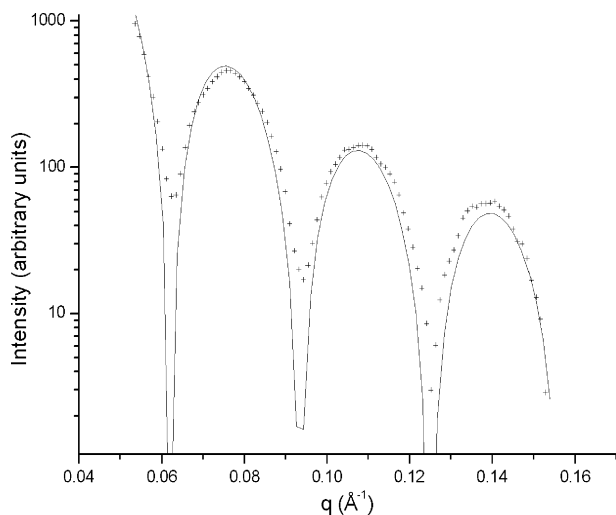


**Figure 3.** Integration of SAXS data along the spike of a 12 g/L SDS foam film, giving 17 nm thickness. The plain line corresponds to the fit of this data with the parameters ( $d$ ,  $e$ , and  $\delta_1/\delta_2$ ) given in the text.

measurements: bamboo foam can remain more than 12 h. It has been shown<sup>18</sup> that those caps induce a pressure difference on both sides of the film, illustrated by a small curvature of the film. The tube was vertical with a fine control of the position by collecting the maximum intensity reflected by a film surface of the bamboo foam. The times of exposition of a film were 5, 10, or 15 min, giving reproducible data.

## Results

**SAXS Data Treatment.** The two-dimensional data have been processed by the FIT2D software.<sup>26</sup> An example of a scattering pattern of a bamboo foam film is presented in Figure 2. Such a result was observed in previous studies.<sup>17,18</sup> It is composed of two contributions: an isotropic one and an anisotropic one. The isotropic contribution, in the shape of circular halos, comes mainly from the Kapton tube. The other contribution illustrated by a

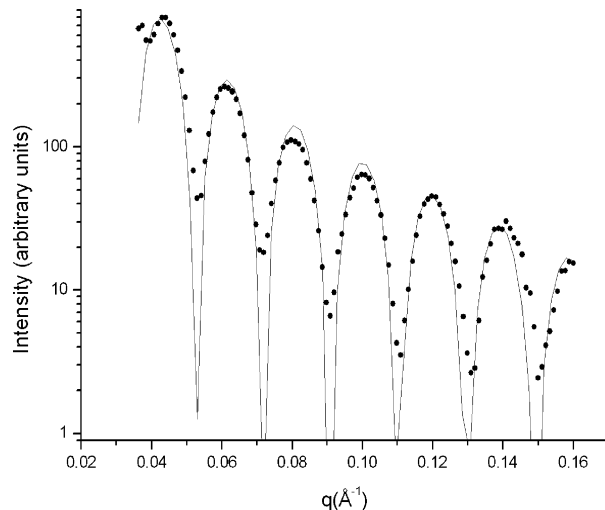


**Figure 4.** Integration of SAXS data along the spike of a 12 g/L SDS foam film, giving 33 nm thickness. The plain line corresponds to the fit of this data with the parameters ( $d$ ,  $e$ , and  $\delta_1/\delta_2$ ) given in the text.

spike is due to reflection of the beam on the curved film surface. The isotropic contribution was measured in the angular part without spike and was subtracted from the whole signal of the anisotropic one, to extract information on thickness and structure from them. We obtain then a specular reflectivity profile in the shape of oscillations superimposed with a  $q^{-4}$  decay, the so-called Kiessig fringes<sup>27</sup> (Figures 3 and 4).

**Fit of the SAXS Data.** A “three-layer” model was selected to refine the data. For this model, the common black film is described as a slice of solution surrounded by two layers of surfactant. Roughness is neglected here because its effect is observed at wider angles than those studied. The shape and the width of the Kiessig fringes are weakly modulated, indicating that the electronic density gradients within the film are weak. However, a single-slab model, corresponding to a homogeneous film, does not provide a suitable fit of the experimental curve. Within kinematical approximation, the specular reflectivity intensity is fitted by the following equation:<sup>28</sup>

$$I(q) \propto \frac{32\pi^2 r_0^2}{q^4} \left[ 2\delta_1 \sin\left(\frac{qe}{2}\right) \cos\left(q\left(\frac{d+e}{2}\right)\right) + \delta_2 \sin\left(\frac{qd}{2}\right) \right]^2 \quad (3)$$

where  $q$  is the scattering vector,  $r_0$  is the classical electron radius,  $\delta_1$  and  $\delta_2$  are the electronic densities of the surfactant (SDS) layer and the solution (aqueous core) layer, respectively,  $e$  is the thickness of the surfactant layer, and  $d$  is the thickness of the solution slice. We made several assumptions in the fitting process. As flux is relatively low as compared to high flux X-ray (synchrotron) sources,<sup>17,18</sup> it is experimentally difficult to have a good precision on the thicknesses and electronic densities simultaneously. According to eq 3 and to limit the number of fitting parameters, we only investigated the ratio  $\delta_1/\delta_2$ . We chose to impose the layer thickness value to 20 Å. This value takes into account the length of SDS molecules with  $\text{CH}_3(\text{CH}_2)_{11}\text{OSO}_3^-$  anions (17 Å) and  $\text{Na}^+$  counterions in the vicinity of the sulfonate heads.<sup>29</sup> The algorithm of the fit (Levenberg–Marquardt) uses a statistical ponderation giving more weight to highest intensity values, that is, first oscillations and tops of the last oscillations.

(27) Kiessig, H. *Ann. Phys.* **1931**, *10*, 769.

(28) Holy, V.; Pietsch, U.; Baumbach, T. *High-Resolution X-Ray Scattering From Thin Films and Multilayers*; Springer-Verlag: Berlin, Heidelberg, New York, 1999.

(29) Bergeron, V. *J. Phys.: Condens. Matter* **1999**, *11*, R215.

(26) Hammersley, A. P. *Scientific software FIT2D*; URL: <http://www.esrf.org/computing/scientific/FIT2D>.

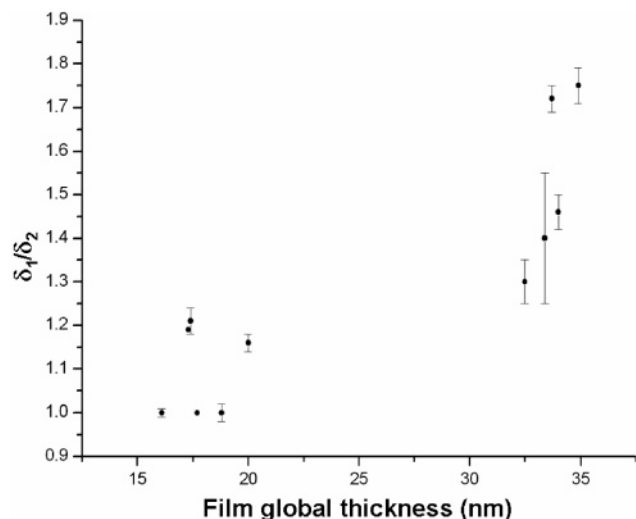


**Figure 5.** Variation of the ratio of the electronic densities  $\delta_1/\delta_2$  between the surfactant layer and the solution slice as a function of SDS foam films thickness.

The error bars for the whole set of parameters are automatically determined by the fitting software ORIGIN 6.0 (Microcal Software, USA) using the defined algorithm, giving a fit quality characterized by chi-squared ( $\chi^2$ ).

Several data have been recorded on SDS bamboo foams, and the refined data were classified into two categories. Figures 3 and 4 represent both kinds of film thickness depending on the foam liquid fraction: Figure 3 for “shaken” foams and Figure 4 for wet foams. For Figure 3, the fitting parameters are  $d + 2e = 200.0 \pm 0.6 \text{ \AA}$  (global film thickness) and  $\delta_1/\delta_2 = 1.06 \pm 0.03$ ,  $\chi^2$  being 7.95. For Figure 4, we found  $d + 2e = 335 \pm 0.9 \text{ \AA}$  and  $\delta_1/\delta_2 = 2.17 \pm 0.14$  with  $\chi^2 = 11.0$ . Several experiments have been performed, and each of them leads to a result that is in good agreement with one of those categories in terms of film thickness. Figure 5 summarizes all of the performed experiments, by presenting the ratio  $\delta_1/\delta_2$  as a function of the film thickness.

**TFPB Results.** Several compression isotherms were carried out on different “fresh” SDS solutions. Without adding salt in our solution, we were able to measure the thickness of common black films only. In the DLVO (Derjaguin Landau Veerwey Overbeek) theory, the equilibrium thickness is known to be determined by a balance between van der Waals dispersion forces and repulsive double-layer overlap forces.<sup>30</sup> Moreover, with such a concentration (5 times higher than cmc), supramolecular forces have a role of great importance in the disjoining pressure value.<sup>31,32</sup> When compressing a film, the formation of a colored spot is observed. The film reaches its equilibrium state quite rapidly, and the spot becomes gray and extends in size. The experimental setup used allows one to measure thickness values for only gray spots (thickness less than 102 nm) and for spot sizes large enough, that is, about 500  $\mu\text{m}$ . The results are summarized in Figure 6. The  $\Pi-e$  isotherm exhibits two branches: one “low-pressure” value (45–55 Pa) branch leading to thickness compromised between 45 and 30 nm and a second “high-pressure” branch (45 to a few 100th Pa) leading to thickness around 20 nm. In this present study, we did not refine the data by the standard DLVO model because we did not seek to define the involved intermolecular forces.

## Discussion

**SDS Film Thickness.** The TFPB results are in good agreement with those found in the literature.<sup>21,33,34</sup> Like numerous ionic surfactants taken beyond their cmc, SDS exhibits different

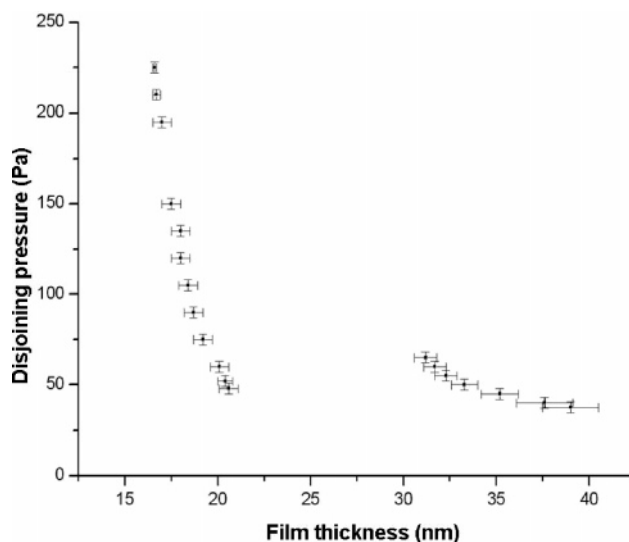


**Figure 6.** Disjoining pressure of a 12 g/L SDS thin film as a function of the film thickness upon a compression.

equilibrium thickness values. This process known as stratification is attributed to structural arrangement of the SDS micelles within the thin film.<sup>21,29</sup> Upon compression, films tend to thin until they reach a critical value for which micelles layers are too close to each other. At this stage, a large amount of micelles is quickly expelled, and the film reaches a new equilibrium thickness.<sup>31</sup> Depending on the concentration of the solution, several branches can be isolated, in our case, two branches.<sup>32</sup>

The thickness values of bamboo foam films measured by SAXS are in good agreement with the TFPB results. The two categories described previously correspond to the two branches of the disjoining pressure isotherm. The X-ray data presented here (resulting approximately from 20 recorded patterns) and elsewhere<sup>17,18</sup> did not give any thickness of film different from that measured by TFPB. Only the thickness of about 30 nm was measured on a bamboo foam.<sup>18</sup> The other thickness of a score of 20 nm was detected on a completely disordered foam, obtained by beating and introduced into a capillary tube.<sup>17</sup> One of the originalities of the work presented here is to have measured on only one bamboo foam these two types of thickness. Mostly, when gently bubbling air in the tube and placing it quick in the X-ray beam (wet foam), we measured thickness of about 33 nm, that is, corresponding to the second branch. To observe foams with thinner films (20 nm), we previously shook the tube to dry the foam. A part of the solution is thus evacuated to be located at the bottom of the tube. The majority of the films present in a bamboo foam have almost the same thickness, that is, 33 or 20 nm. Experiments with a single film taken randomly in the foam bursting the other films have also given the same results, suggesting that films behave as if they are isolated. Sometimes, a film thickness of 20 nm can be detected in a film sequence of 33 nm. For very long experiment times of about an hour, we observed some rare transitions from 33 to 20 nm. Nevertheless, we are not able to conclude if the transition occurs the same way for every foam or if it was due to small vibrations of the setup. This explains the results on disordered

(30) Israelachvili, J. *Intermolecular and Surface Forces*; Academic Press Inc.: San Diego, CA, 1998.

(31) Pollard, M. L.; Radke, C. J. *J. Chem. Phys.* **1994**, *101*, 6979.

(32) Kralchevsky, P. A.; Denkov, N. D. *Chem. Phys. Lett.* **1995**, *240*, 385.

(33) Cascao, Pereira, L. G.; Johansson, C.; Blanch, H. W.; Radke, C. J. *Colloids Surf., A* **2001**, *186*, 103.

(34) Yaros, H. D.; Newman, J.; Radke, C. J. *J. Colloid Interface Sci.* **2003**, *262*, 442.

foams.<sup>16,17</sup> In that case, drainage makes foam liquid fraction less than 10% very rapidly, and hence capillary pressure becomes high.

These observations led us to focus on the disjoining pressure value of films within a bamboo foam. It is indeed surprising to measure film thicknesses that are commonly attributed to metastable state of the films, that is, which only exist for small values of the disjoining pressure. For thicker films, the disjoining pressure of the larger film is estimated around 40 Pa (Figure 6) and seems very stable over a long time. SDS is taken at high concentration in regard to its cmc. Thus, surface tension of the flat film and that of the menisci should be equal because there is no contact angle in the transition meniscus–film. As the pressure difference between two bubbles is of the order of less than 1 Pa,<sup>18</sup> the disjoining pressure is attributed to capillary pressure in the Plateau border, the menisci around the film.

On the other hand, mechanically evacuating the water out from the foam allows the film to reach thickness, which requires typically 100 Pa. This is obviously accompanied by an increase in the capillary pressure and therefore a decrease in the Plateau border radius.

These observations led to the conclusion that bamboo foam films may be seen as independent isolated films with no collective effect. This can be quite surprising as collective effects have been seen when moving a bamboo foam in a horizontal tube.<sup>9,10</sup> This case refers to experiments on ordered foams flowing through a narrow channel, for which a wetting film spreads all along the wall and ensures connectivity between films. In our case corresponding to a bamboo drained foam in a vertical tube, the wetting film has not been observed by SAXS with the experimental conditions ( $q$ -range, exposition time, flux X-ray source). A wetting film like air/liquid/Kapton with a thickness below 5 nm or a weak electronic density variation cannot be here detected. From this study, we cannot conclude that the wetting film exists or not. Recent experiments on drainage of bamboo foams<sup>13</sup> thus showed that at the end of drainage all films are separated from each other.

**Geometrical Properties of a Bamboo Foam Film at the End of Free Drainage.** We observed that a wet bamboo foam reaches its equilibrium state by having a film thickness of 33 nm. As the tube radius is close to the capillary length  $l_c$  defined as  $[\gamma/(\rho g)]^{1/2}$  (in our case  $l_c = 1.9$  mm), the cross section of the Plateau border features two arcs of circles. If we assume a zero contact angle at the tube wall, the drainage flow in the bamboo foam is expected to stop when we have a Plateau border's size (size of a meniscus) of twice the capillary length.<sup>13</sup> Hence, capillary pressure  $P_c$  exerted by the meniscus should be  $2\gamma/l_c = 37.5$  Pa. This value of capillary pressure is in good agreement with the disjoining pressure needed to obtain a film of 33 nm. Nevertheless, by image analysis (by photographing the film), the Plateau border size is found to be  $1.6 \pm 0.1$  mm instead of 3.8 mm. Thus, wettability of the tube must be taken into account. By a simple optical measurement (visualization of a drop deposited on a support), the contact angle  $\theta$  between 12 g/L SDS and Kapton has been found to be  $38 \pm 4^\circ$ . Assuming no change in the curvature of the Plateau border, a simple calculation gives a Plateau border size  $Y$  to be  $Y = 2l_c(1 - \sin \theta)$  (Figure 7). We would then expect  $Y$  to be  $1.46 \pm 0.12$  mm, which is in good agreement with our measured value. To confirm this fact, we also estimated a value  $X$ , which corresponds to the length of the Plateau border. It is difficult to determine precisely the point where the film does not seem curved anymore. Nevertheless, our measurements led to a value  $X = 1.5 \pm 0.2$  mm. With our modeling of the curvature of the Plateau border, we would expect this

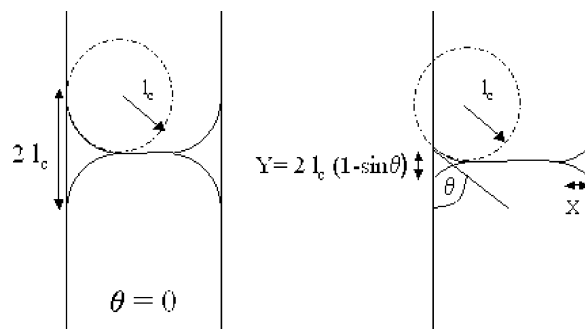


**Figure 7.** Scheme of the geometry of a bamboo foam film within a tube. On the right side, we assume a zero contact angle between the liquid menisci and the tube. The left side describes the case of a nonzero contact angle and explains the parameter  $Y$  used in the text.  $X$  corresponds to the length of the Plateau border.

value to be  $X = l_c \cos \theta = 1.5 \pm 0.1$  mm. Once again, these values are very close. Note that this treatment remains true only for foams at rest during and after drainage.

It appears then that the radius of curvature of Plateau borders in a bamboo foam after drainage and without external perturbations always equals the capillary length even for nonzero contact angle. We thus can predict the thickness of surfactant films of bamboo foams at rest. We explain in the same time how it is possible to observe metastable state of thin films over a long time.

**Electronic Density Variations.** Figure 5 shows the ratio of electronic densities versus the film thickness obtained by refined SAXS data. Although error bars seem large, one can observe a clear tendency. Larger films exhibit a ratio  $\delta_1/\delta_2$  higher than thinner films. As expected, electronic density of the surfactant layer is always higher than the solution slice's one,<sup>35–38</sup> but we highlighted a variation of the relative density with the thickness. Because of the high concentration of the solution, the interfacial concentration may be constant for the two states of the film. The thermodynamic definition of the interfacial surface tension  $\gamma_i = \gamma - \int_{-\infty}^h \Pi(h) dh$ , where  $\gamma_i$  is the surface tension of one interface of the film, leads to a value approximately equal to the surface tension of a single air/liquid interface. For fitting the SAXS data, we have fixed the SDS surfactant layer thickness to 20 Å. Yet this value could change upon the thickness transition. We could explain this variation by a change in the concentration of the aqueous core. Ionic strength would thus increase and the counterion layer around the surfactant would thin by a decrease of the Debye length. Another point of view of this phenomenon is that the surfactant layers' charge overlap becomes stronger. This could induce a higher repelling of the surfaces compressing the counterions layer. The stability of the thinner branch of the disjoining pressure isotherm (Figure 6) is thus dominated by electrostatic double layer forces. Attempts at fitting the SDS surfactant layer thickness while keeping the electronic densities ratio led to variations of this thickness of about 1 Å. However, the assumptions of explanation remain difficult to check with our setup. The maximum of  $q$  is  $0.019 \text{ \AA}^{-1}$ , which prevents the study in details of distances lower than 33 Å.

## Conclusions

SAXS experiments on bamboo drained films stabilized with SDS above the cmc (12 g/L) highlighted the existence of two kinds of thickness. Whatever the film position in the tube, the

- (35) Benattar, J. J.; Schalchli, A.; B elorgey, O. *J. Phys. I France* **1992**, *2*, 955.  
 (36) B elorgey, O.; Benattar, J. *J. Phys. Rev. Lett.* **1991**, *66*, 313.  
 (37) Sentenac, D.; Dean, D. S. *J. Colloid Interface Sci.* **1997**, *196*, 35.  
 (38) Bresme, F.; Faraudo, J. *Langmuir* **2004**, *20*, 5127.

thickness remains the same and is comparable to that measured on an isolated film. TFPB data clearly showed two branches in the disjoining pressure isotherms. The transition from one thickness to another can be carried out by drainage resulting from a mechanical vibration. It results that a bamboo foam is simply an assembly of independent films. A discussion on the geometry of the Plateau border is proposed to explain the stability of the foam films.

The refinement of the X-ray data by using the simple “three-layer” model showed an unusual behavior of the electronic densities. The electronic density of the SDS layer with respect to that of the solution layer decreases according to the total thickness of film. Assuming that the air/water interface is completely saturated, it seems that the thinning of film affects the electronic distribution of the surfactant layer. It may come from a SDS concentration increases in the aqueous core; that is, SDS micelles would approach and make water evacuate. Another possibility is that the description of the SDS layer to the air/

liquid interface is too idealized. The  $\text{Na}^+$  counterions can approach the  $\text{CH}_3(\text{CH}_2)_{11}\text{OSO}_3^-$  anions. Up to now, only measurements on isolated Newton black films<sup>35,36</sup> (a sandwich structure containing no aqueous core) have been performed, and the resulting data have been compared to molecular dynamics studies.<sup>39,40</sup> The following stage of work would be to stabilize Newton black films in a bamboo foam in the presence of high salt concentration and to extract from it the electronic density starting from high-resolution X-ray data.

**Acknowledgment.** We acknowledge funding from Region Bretagne. We want to thank A. Colin (LOF, Bordeaux-I, France) for helping us mount the TFPB apparatus, and I. Cantat and A. Saint-Jalmes for fruitful discussions.

LA701738Z

---

(39) Gamba, Z.; Hautman, J.; Shelley, J. C.; Klein, M. L. *Langmuir* **1992**, *8*, 3155.

(40) Jang, S. S.; Goddard, W. A. *J. Phys. Chem. B* **2006**, *110*, 7992.